Neuron, Vol. 31, 581–591, August 30, 2001, Copyright ©2001 by Cell Press

Munc18-1 Promotes Large Dense-Core Vesicle Docking

Thomas Voets,[1,5,6] Ruud F. Toonen,[3] Elisabeth C. Brian,[3] Heidi de Wit,[3] Tobias Moser,[1,2] Jens Rettig,[1,7] Thomas C. Südhof,[4] Erwin Neher,[1] and Matthijs Verhage[3,5]

[1]Department of Membrane Biophysics
Max-Planck-Institute for Biophysical Chemistry
Am Fassberg 11
37077 Göttingen

[2]Department of Otolaryngology
Göttingen University Medical School
Robert-Koch-Strasse
37073 Göttingen
Germany

[3]Molecular Neuroscience-Rudolf Magnus Institute
University of Utrecht Medical Center
Universiteitsweg 100
3584 CG Utrecht
Netherlands

[4]Department of Molecular Genetics and
Howard Hughes Medical Institute
Center for Basic Neuroscience
University of Texas Southwestern Medical Center
6000 Harry Hines Boulevard
Dallas, Texas 75235

Summary

Secretory vesicles dock at the plasma membrane before Ca^{2+} triggers their exocytosis. Exocytosis requires the assembly of SNARE complexes formed by the vesicle protein Synaptobrevin and the membrane proteins Syntaxin-1 and SNAP-25. We analyzed the role of Munc18-1, a cytosolic binding partner of Syntaxin-1, in large dense-core vesicle (LDCV) secretion. Calcium-dependent LDCV exocytosis was reduced 10-fold in mouse chromaffin cells lacking Munc18-1, but the kinetic properties of the remaining release, including single fusion events, were not different from controls. Concomitantly, mutant cells displayed a 10-fold reduction in morphologically docked LDCVs. Moreover, acute overexpression of Munc18-1 in bovine chromaffin cells increased the amount of releasable vesicles and accelerated vesicle supply. We conclude that Munc18-1 functions upstream of SNARE complex formation and promotes LDCV docking.

Introduction

The release of neurotransmitter from nerve terminals and hormones from neuroendocrine cells involves the fusion of vesicles with the plasma membrane in response to increases in the intracellular Ca^{2+} concentration ($[Ca^{2+}]_i$) (Zucker, 1996). Before secretory vesicles can fuse, they first attach to the plasma membrane ("docking") and undergo maturation that makes them competent for fusion ("priming") (Robinson and Martin, 1998). Over the last decades, biochemical and genetic approaches have identified a vast amount of proteins that regulate vesicle trafficking and fusion, but the exact function of most of these proteins remains unclear (Fernandez-Chacon and Südhof, 1999; Augustine et al., 1999; Lin and Scheller, 2000). Membrane fusion reactions in all eukaryotic cells appear to involve a conserved family of proteins termed "SNAREs" (soluble N-ethylmaleimide-sensitive fusion protein [NSF]-attachment protein [SNAP] receptors) (Bennett and Scheller, 1993; Söllner et al., 1993; Hay and Scheller, 1997; Chen and Scheller, 2001). The SNAREs involved in neurosecretion include the plasma membrane-associated proteins Syntaxin-1 and SNAP-25 and the vesicular protein Synaptobrevin (also known as VAMP). The fundamental role of these proteins in neurosecretion is underlined by the fact that the potent inhibition of neurotransmission by various botulinum and tetanus toxins is due to the ability of these toxins to specifically cleave the different SNARE proteins (Niemann et al., 1994). The assembly of SNARE monomers into a parallel four-helix bundle, the *trans*-SNARE complex, is believed to be a crucial step in the exocytic fusion reaction in that it brings vesicle and plasma membrane in close apposition (Weber et al., 1998; Sutton et al., 1998; Chen et al., 1999; Brunger, 2000).

Munc18-1 (also known as nSec1, Munc18-a, and rbSec 1) is a mammalian member of the Sec1/Munc18-related proteins (SM proteins), a conserved family of proteins, related to *C. elegans* unc18 and *S. cerevisiae* Sec1p, that appear to be involved in all eukaryotic membrane fusion reactions (Jahn, 2000). Since most SM proteins interact specifically and with high affinity to Syntaxin-like SNAREs (Hata et al., 1993; Pevsner et al., 1994b; Grabowski and Gallwitz, 1997; Nichols et al., 1998), which is mutually exclusive of SNARE complex formation in most species (Pevsner et al., 1994b; Dulubova et al., 1999; Yang et al., 2000; but see Carr et al., 1999), it has been suggested that SM proteins are negative regulators of secretion. In agreement with this idea are studies showing a reduction of neurotransmitter release in *Drosophila* and squid after introduction of the respective Munc18-1 orthologs Rop and s-Sec1 (Schulze et al., 1994; Dresbach et al., 1998). In contrast, a study on regulated exocytosis in permeabilized chromaffin and PC12 cells provided evidence against an acute inhibitory role for Munc18-1 (Graham et al., 1997). Moreover, secretion is blocked in *S. cerevisiae* Sec1p mutants (Novick et al., 1980) and in *Drosophila* Rop null mutants (Harrison et al., 1994), and synaptic transmission is completely inhibited in mouse Munc18-1 null mutants (Verhage et al., 2000), suggesting an essential, positive role for SM proteins in membrane fusion. Hence, although the general importance of SM proteins in secretion is

[5]Correspondence: thomas.voets@med.kuleuven.ac.be (T.V.), m.verhage@med.uu.nl (M.V.)

[6]Present address: Laboratorium voor Fysiologie, Katholieke Universiteit Leuven, Campus Gasthuisberg O&N, B-3000 Leuven, Belgium.

[7]Present address: Physiologisches Institut, Universität des Saarlandes, D-66421 Homburg/Saar, Germany.

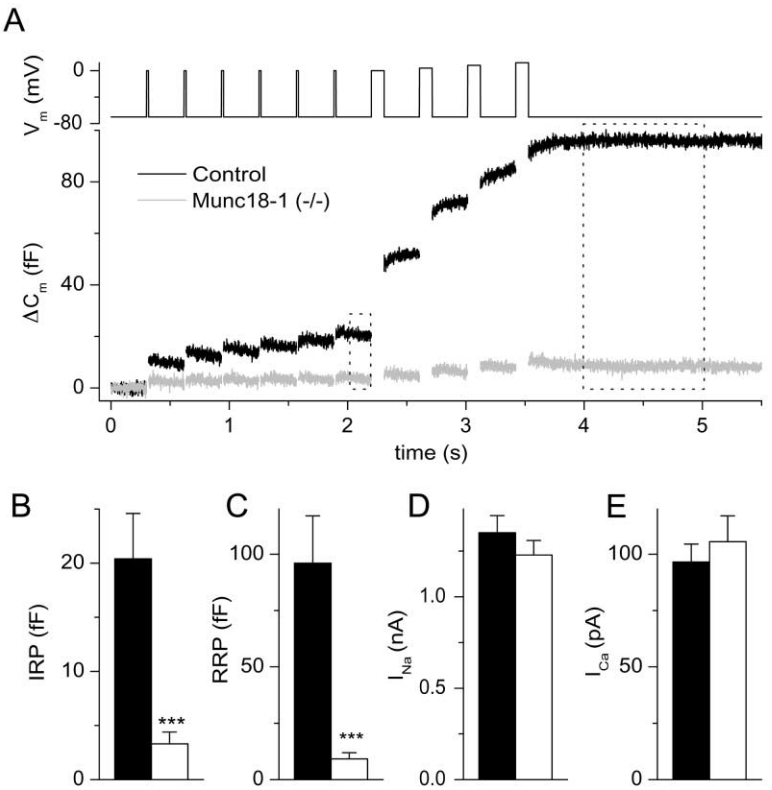

Figure 1. Reduced Depolarization-Induced Secretion in Chromaffin Cells from Munc18-1 Null Mutants

(A) Voltage protocol (top) and resulting average capacitance increase (ΔC_m) in chromaffin cells from control (24 cells from four animals) and Munc18-1 null mutant (27 cells from five animals) mice.

(B) Comparison of the size of the IRP, determined as the average ΔC_m during the time period indicated by the leftmost dashed rectangle in (A).

(C) Comparison of the size of the RRP, determined as the average ΔC_m during the time period indicated by the rightmost dashed rectangle in (A). Note that the RRP includes the IRP (Voets et al., 1999).

(D) Comparison of the amplitude of the voltage-gated sodium currents, defined as the peak inward current for a depolarization to 0mV.

(E) Comparison of the amplitude of the voltage-gated calcium currents, defined as the inward current after 10 ms depolarization to 0mV.

(B–E) Solid bars represent controls, and open bars represent Munc18-1 null mutant cells. Error bars indicate the SEM. Significant differences (Student's t test) are indicated (***$p < 0.001$).

undisputed, their exact molecular function remains elusive.

Calcium-dependent exocytosis of LDCVs in chromaffin cells can be studied at high temporal resolution using membrane capacitance measurements and carbon fiber amperometry, which allows a detailed quantitative analysis of the different steps in the secretory pathway (Neher, 1998; Voets et al., 1999; Xu et al., 1999; Voets, 2000). In this study, we established a slice preparation from embryonic adrenal glands, which allowed the use of these powerful techniques to study LDCV secretion in genetically engineered mice that die at birth. We show that the exocytic response to depolarizing pulses and to flash photolysis of caged calcium is severely inhibited but not abolished in chromaffin cells from Munc18-1 null mutant mice. Kinetic analysis of the remaining response indicates that the fusion step itself is not affected, suggesting that the recruitment of fusion-competent vesicles is impaired. Ultrastructural analysis of null mutant chromaffin cells revealed a strong, selective reduction of the number of LDCVs attached to the plasma membrane. Finally, overexpression of Munc18-1 in isolated bovine chromaffin cells increased both the amount of fusion-competent vesicles and the rate of vesicle supply. Taken together, these data point toward an essential, positive role for Munc18-1 in LDCV docking.

Results

Munc18-1-deficient mice are completely paralyzed and die immediately after birth, presumably due to their paralysis (Verhage et al., 2000). To avoid possible indirect effects of the paralyzed state on the secretory phenotype, we analyzed adrenal glands from E18 embryos that were obtained by caesarean section of pregnant females from timed heterozygous matings. To investigate the effect of Munc18-1 deletion on depolarization-induced secretion, chromaffin cells were stimulated with a voltage protocol consisting of six 10 ms depolarizations followed by four 100 ms depolarizations delivered 300 ms apart (Figure 1A, top). We have previously shown that the 10 ms depolarizations cause the fusion of the immediately releasable pool (IRP), which corresponds to a fraction of the readily releasable vesicles that are closely associated with Ca^{2+} channels. The subsequent 100 ms depolarizations elicit fusion of the remainder of the readily releasable pool (RRP) (Voets et al., 1999). Control chromaffin cells responded to such depolarizing trains with robust increases in membrane capacitance (C_m; Figures 1A–1C). In contrast, the secretory response was drastically reduced in chromaffin cells from Munc18-1 null mutant embryos (Figures 1A–1C). Controls and Munc18-1 null mutants were indiscernible with respect to resting membrane capacitance, voltage-gated Na^+ and Ca^{2+} currents, basal $[Ca^{2+}]_i$, and stimulus-evoked $[Ca^{2+}]_i$ transients (Figures 1D–1E and data not shown).

In principle, the strong reduction in depolarization-induced secretion in the absence of Munc18-1 could be due to an impaired coupling between vesicles and Ca^{2+} channels. To test this, we by-passed Ca^{2+} channels and stimulated exocytosis with step-wise, uniform increases in $[Ca^{2+}]_i$ induced by flash photolysis of caged calcium. Two phases are discriminated in the exocytic response to flash photolysis of caged calcium: the exocytic burst, which is defined as the first second of the flash response and corresponds to exocytosis of fusion-competent

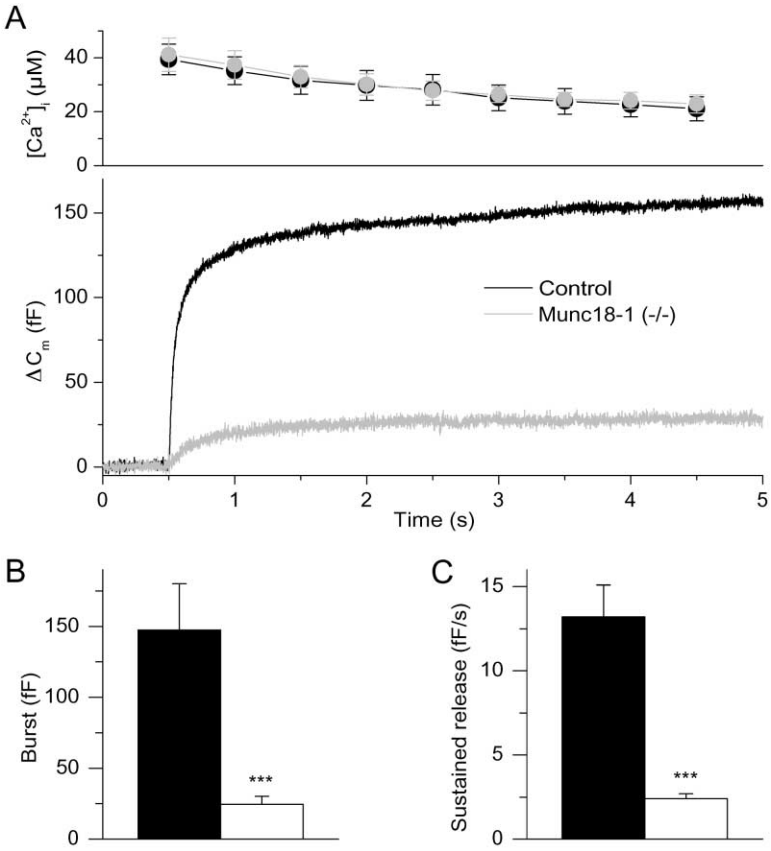

Figure 2. Reduced Exocytosis in Adrenal Chromaffin Cells from *Munc18-1*$^{-/-}$ Mice after Flash Photolysis of Caged Calcium

(A) Average $[Ca^{2+}]_i$ (top) and ΔC_m in response to flash photolysis of NP-EGTA in control (17 cells from four animals; black line and symbols) and Munc18-1 null mutant (19 cells from five animals; gray line and symbols) cells.

(B) Comparison of the exocytic burst in control and Munc18-1 null mutant cells. The exocytic burst was determined as the ΔC_m 1 s after the flash.

(C) Comparison of the rate of sustained release, which was defined as the slope of the C_m trace between 2 and 5 s after the flash.

(B and C) Solid bars represent controls, and open bars represent Munc18-1 null mutant cells. Error bars indicate the SEM. Significant differences (Student's t test) are indicated (***$p < 0.001$).

vesicles, and the sustained component, which reflects the recruitment of new vesicles immediately followed by fusion. Both the exocytic burst and the sustained component of secretion were strongly reduced in the Munc18-1 null mutants (Figures 2A–2C). These differences cannot be explained by differences in $[Ca^{2+}]_i$ at the release sites (Figure 2A, top). Hence, the secretory defect in the absence of Munc18-1 does not reflect alterations in the coupling between vesicles and Ca^{2+} channels.

Analogous to previous work (Voets et al., 1999), two kinetic components could be distinguished in the exocytic burst from control cells: a fast component (τ_{fast} = 28.9 ± 4.0 ms; A_{fast} = 93 ± 23 fF), which corresponds to the fusion of the RRP (including the immediately releasable pool, see above), and a slower component (τ_{slow} = 357 ± 64 ms; A_{slow} = 63 ± 14 fF), which reflects the slower, parallel fusion of the slowly releasable pool (SRP). Together, the RRP and SRP are thought to be those vesicles that are connected to the plasma membrane through *trans*-SNARE complexes. The transition between SRP and RRP is rapid ($\tau \sim 4$ s) (Voets et al., 1999) and may represent the interconversion of the SNARE complex between a loose and a tight state (Xu et al., 1999). Although most C_m responses from the null mutants were too small to allow such a detailed kinetic analysis, two kinetic components could be distinguished in the largest responses in the null mutant cells, yielding values for τ_{fast} and τ_{slow} of 43.8 ± 14.3 ms and 334 ± 120 ms, respectively (n = 4; values not significantly different from control). From this, we conclude that Munc18-1 deletion had no major effect on the fusion kinetics of the different fusion-competent vesicle pools.

To test whether the reduction in secretion observed in the Munc18-1 null mutants is due to a shift in the Ca^{2+} sensitivity for exocytosis, flash intensity was varied, resulting in a broad range of postflash $[Ca^{2+}]_i$ levels. Control cells already displayed robust C_m responses for postflash $[Ca^{2+}]_i$ levels above 6 μM, and higher $[Ca^{2+}]_i$ levels caused faster fusion rates without affecting the amplitude of the exocytic burst (see also Voets, 2000). In contrast, flash responses remained strongly reduced in the null mutants, even for postflash $[Ca^{2+}]_i$ levels up to 100 μM (data not shown). Taken together, our results strongly suggest that the Munc18-1 null mutation results in a severe reduction of the number of releasable vesicles.

Munc18-1 null mutant chromaffin cells showed a small but significant increase in C_m in response to depolarization-induced and flash-induced elevations in $[Ca^{2+}]_i$, while previous studies showed that small synaptic vesicle exocytosis in null mutant CNS neurons was completely blocked (Verhage et al., 2000). To ascertain that the above-described responses indeed reflect LDCV secretion and not some unspecific changes in C_m, we directly measured catecholamine release using carbon fiber amperometry. This technique allows recording of individual exocytic events as fast amperometric spikes, which correspond to electrooxidation of the catecholamines contained within a single LDCV (Chow et al., 1992). When stimulated with a depolarizing extracellular solution (70 mM K^+), amperometric spikes could be re-

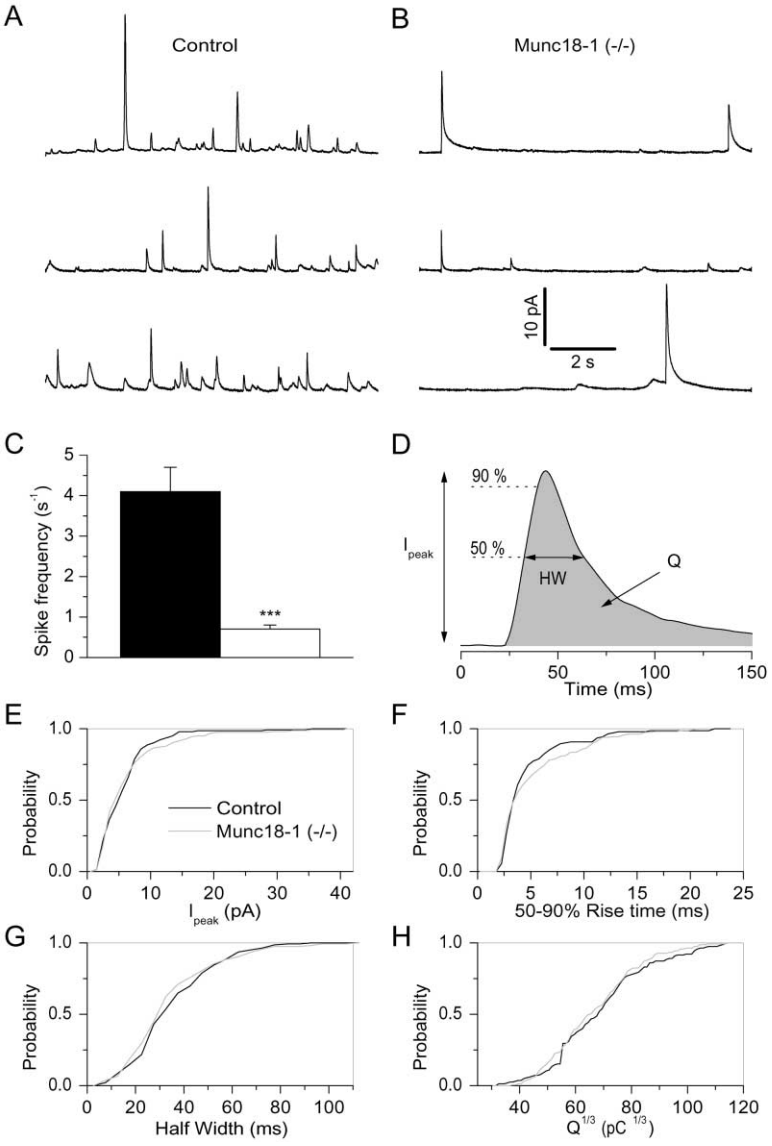

Figure 3. Single Fusion Events Measured by Carbon Fiber Amperometry Are Normal in *Munc18-1*$^{-/-}$ Mice

(A and B) Examples of amperometric recordings in control (A) and *Munc18-1*$^{-/-}$ slices (B) during stimulation with a 70 mM K^+ solution.

(C) Comparison of the average spike frequency during high-K^+ stimulation for control (solid bar, six cells from two animals) and Munc18-1 null mutant (open bar, seven cells from two animals) cells. (***$p < 0.001$; Student's t test).

(D) Example of the detailed analysis of a single spike, indicating peak current (I_{peak}), current integral (Q), 50%–90% rise time, and the spike half-width (HW).

(E–H) Cumulative probability plots comparing single spikes from control (165 spikes) and *Munc18-1*$^{-/-}$ cells (146 spikes) ($p > 0.2$ for all parameters; Kolmogorov-Smirnoff test).

corded from chromaffin cells in slices from both control and null mutant mice (Figures 3A and 3B). The spike frequency was strongly reduced in the null mutants (Figure 3C). Hence, the amperometric measurements of catecholamine release confirm that the Munc18-1 deletion results in a severe reduction but not a full inhibition of LDCV secretion.

To investigate whether Munc18-1 regulates the kinetic properties of single LDCV fusion events, we determined the peak current (I_{peak}), current integral (Q), 50%–90% rise time, and the spike half-width (Figure 3D) for individual spikes. The frequency distributions for these different parameters revealed no significant differences between control and null mutant cells (Figures 3E–3H). Manipulations that affect late stages in the release process (e.g., fusion pore opening and expansion or release of catecholamine from the vesicular matrix) are expected to affect the rise time and half-width of single spikes. Therefore, our data argue against a late function for Munc18-1 in LDCV secretion, as has been recently proposed (Fisher et al., 2001). Moreover, the lack of effect on I_{peak} or Q indicates that Munc18-1 is not involved in the loading of LDCVs with catecholamine.

To test whether the reduction in releasable vesicles in the null mutants resulted from a change in the number of vesicles or their distribution, we performed an electron microscopic analysis of the adrenals from wild-type and Munc18-1 null mutant E18 littermates. At this stage, certain areas of the CNS of these mutants showed prominent cell death (Verhage et al., 2000), but evaluations of the adrenal glands with light microscopy and low-power electron microscopy revealed no morphological differences between control and null mutants (data not shown). At this developmental stage, the chromaffin cells in control adrenals are not completely filled with LDCVs as in mature chromaffin cells (for example, see Gorgas and Böck, 1976; Ashery et al., 2000). Instead, a limited number of vesicles are present, approximately 40 per random cross-section, which are mostly aligned at the plasma membrane (Figures 4A and 4B). In con-

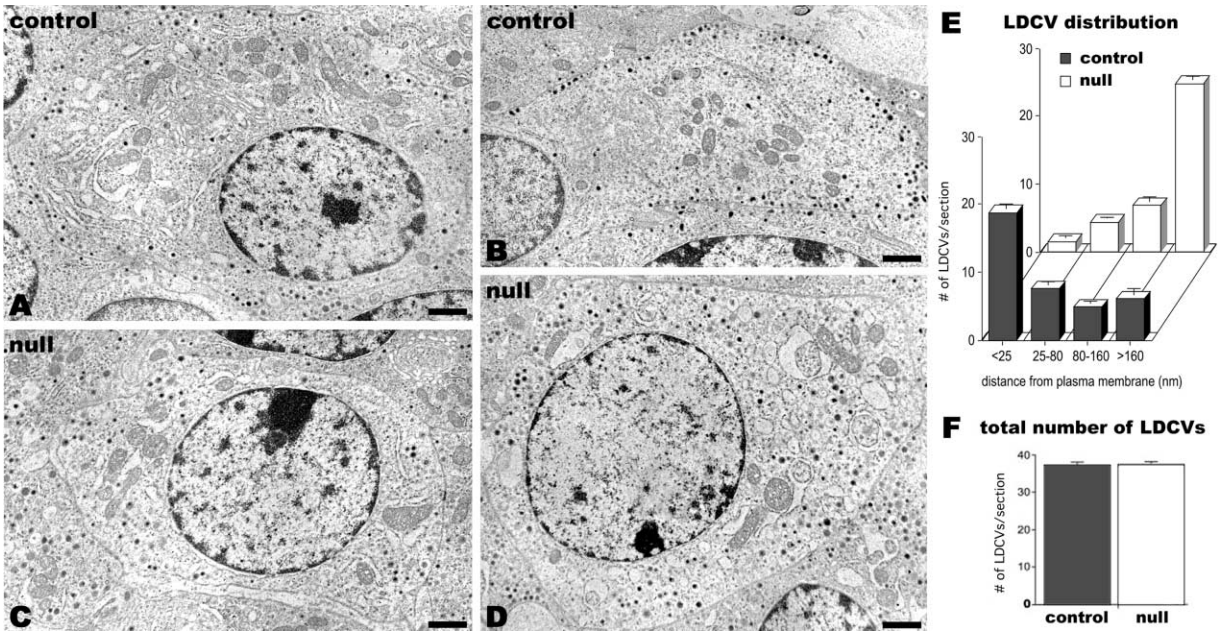

Figure 4. The Munc18-1 Deletion Leads to a Specific Defect in LDCV Docking

(A–D) Two typical examples of micrographs of adrenal sections from wild-type (A and B) and null mutant (C and D) littermates at E18. LDCVs are aligned at the cell surface in wild-type cells (A and B), whereas they are dispersed throughout the cytoplasm in mutant cells (C and D). Bar indicates 1 μm.

(E) Distribution of LDCVs inside chromaffin cells in control (filled bars) and null mutant (open bars) adrenal slices. LDCVs were categorized in four bins according to their distance from the plasma membrane. For both groups, 60 randomly selected chromaffin cells from three different animals were analyzed. Error bars indicate SEM. Differences in the first and last bin were significant between the two groups ($p < 0.003$; Student's t test).

(F) Total numbers of vesicles per section in control (filled bars) and null mutant (open bars) adrenal slices.

trast, the Munc18-1 null mutant chromaffin cells showed a clearly different distribution of LDCVs, with most vesicles being dispersed throughout the cytoplasm (Figures 4C and 4D). Quantification of the LDCV distribution revealed an ~10-fold reduction of docked LDCVs (i.e., vesicles within 25 nm of the plasma membrane, see Steyer et al., 1997) and an ~4-fold increase in the amount of LDCVs scattered throughout the cytoplasm in the Munc18-1 null mutants (Figure 4E). However, the total number of vesicles was identical in control and null mutant chromaffin cells (Figure 4F). Moreover, we occasionally observed so-called "omega-shaped" structures in the mutant chromaffin cells reflecting fusing vesicles (data not shown), confirming that a small number of LDCVs are still competent to undergo membrane fusion.

We tested for changes in the levels of synaptic proteins in the mutant adrenal glands, using Western blotting. As expected, Munc18-1 levels were reduced in the heterozygous mice and undetectable in null mutants (Figure 5A). Cellular levels of Syntaxin-1A/B were decreased ~2-fold in the null mutants, whereas SNAP-25 and Synaptobrevin protein levels were unaltered (Figure 5A). The levels of control proteins CaMKII (α subunit) and VCP were also similar between control and null mutant adrenals (Figure 5A). Adrenal glands express another Munc18 isoform, Munc18c (Tellam et al., 1995), and its expression levels were not significantly altered in the null mutants (Figure 5B). Moreover, in situ hybridization experiments in adrenal glands from newborn and adult mice revealed that Munc18-1 is primarily expressed in the medullary chromaffin cells, whereas Munc18c is mainly restricted to the adrenal cortex (data not shown).

The above results indicate that the chronic absence of Munc18-1 leads to a substantial reduction in the number of releasable vesicles and an equally severe deficiency in the amount of morphologically docked LDCVs, suggesting that Munc18-1 is a positive regulator of LDCV secretion. To confirm these findings in a more acute experiment, we tested whether the opposite situation, Munc18-1 overexpression, would indeed enhance secretion. We transfected isolated bovine chromaffin cells, using the Semliki Forest Virus expression system (Ashery et al., 1999), containing the DNA coding for Munc18-1 and for green fluorescent protein coupled via an internal ribosomal entry site. This technique allows straightforward detection of overexpressing cells based on their green fluorescence, without interfering with Munc18-1 function. Western blot analysis revealed that the level of Munc18-1 protein was at least ten times higher in transfected chromaffin cells than in nontransfected controls, notably without detectable changes in the level of Syntaxin-1 protein (data not shown). The C_m increase after flash photolysis of caged calcium was markedly larger in Munc18-1-overexpressing chromaffin cells than in nontransfected controls (Figure 6A). Both the exocytic burst (Figure 6C) and the rate of sustained release (Figure 6D) were significantly increased. Thus, overexpression of Munc18-1 leads to both a larger

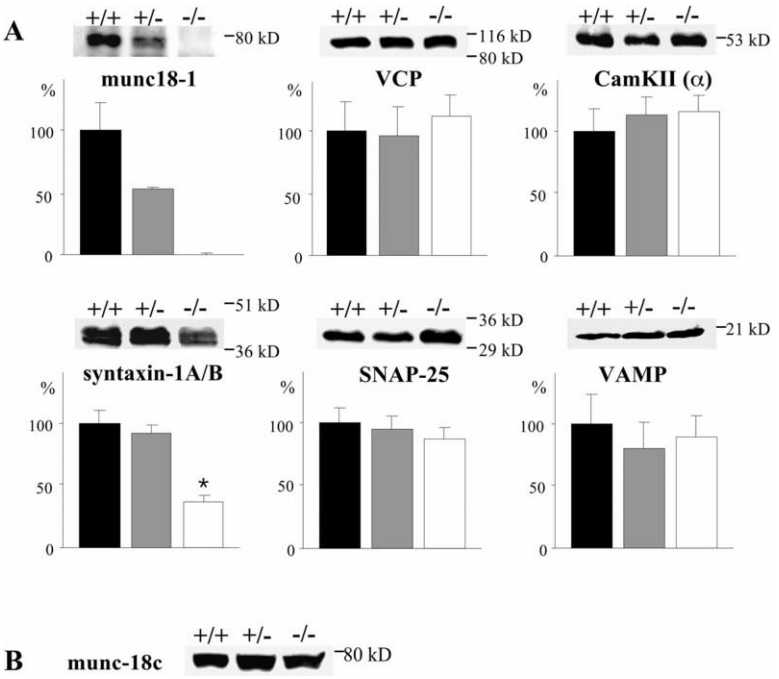

Figure 5. Reduced Syntaxin-1 Protein Levels in Adrenals from Munc18-1-Deficient Mice

(A) Quantification of immunoblot analyses of adrenal protein levels in wild-type (+/+, black bar), heterozygous (+/−, gray bar), and homozygous (−/−, white bar) mice (E18). Results are expressed as means + SEM from six independent adrenal preparations. Example immunoblots are also shown (top). Overall group differences were analyzed using an ANOVA. Differences between wild-types, heterozygotes, and homozygotes were analyzed using a Student's t test with Bonferroni correction (*$p < 0.05$).

(B) Immunoblot analysis of Munc18c protein levels in adrenals from wild-type, heterozygous, and homozygous mice (E18).

amount of fusion-competent vesicles and a more rapid vesicle supply. In agreement with an enhanced vesicle supply, we found that the secretory response to a second flash, applied 120 s after the first flash, was still larger in Munc18-1-overexpressing cells (Figure 6B). Again, both the exocytic burst and the rate of sustained release were significantly increased in comparison with controls (Figures 6C and 6D). Secretory responses remained enhanced in Munc18-1-overexpressing cells for subsequent (third and fourth) flashes (data not shown), although cells from both groups displayed significant secretory run down after the second or third flash. Note that overexpression of GFP alone did not cause any increase in the amplitude of the exocytic burst or the rate of sustained release (data not shown; see also Ashery et al., 1999, 2000). Detailed kinetic analysis of single flash responses from control and Munc18-1-overexpressing cells revealed no differences in the time constants for the two kinetic components of the burst (Figures 6E and 6F). This confirms that the level of Munc18-1 expression does not influence the kinetics of vesicle fusion from either the SRP or RRP. Moreover, the relative contribution of the fast and the slow kinetic component did not change significantly (Figure 6G), indicating that Munc18-1 does not affect the equilibrium between the SRP and the RRP. Taken together, we conclude that Munc18-1 overexpression leads to a persistent enhancement of the supply of fusion-competent LDCVs, without affecting the kinetics of the actual fusion reactions.

Discussion

In this study, we investigated the role of Munc18-1 in Ca^{2+}-dependent secretion from adrenal chromaffin cells. These cells release catecholamines through the fusion of LDCVs with the plasma membrane using the same conserved fusion machinery that functions in neurotransmitter release (Morgan and Burgoyne, 1997). Chromaffin cells offer the advantage that exocytosis can be assayed at high temporal resolution on the single-cell level, using membrane capacitance measurements and carbon fiber amperometry (Neher, 1998), while cellular protein levels can be manipulated chronically by genetic manipulation or acutely by viral transfection, and vesicle distribution can be studied using electron microscopy.

Using these techniques, we identified two related and specific defects in Munc18-1-deficient chromaffin cells, namely in the number of vesicles that can be stimulated to secrete and in the number of morphologically docked vesicles. At the same time, many general features of chromaffin cell function appeared to be unaltered, including general morphology, vesicle biogenesis, resting membrane capacitance, voltage-gated Na^+ and Ca^{2+} currents, basal $[Ca^{2+}]_i$, and stimulus-evoked $[Ca^{2+}]_i$ transients. In addition, a number of specific features of the secretion process were analyzed, allowing us to narrow down the site of action of Munc18-1 in this process. First, our finding that the reduction in secretion was independent of the mode of stimulation (i.e., voltage-dependent Ca^{2+} influx versus flash photolysis of caged calcium) argues against a role in the coupling between vesicles and Ca^{2+} channels. Second, our finding that the reduction in secretion could not be overcome by increasing the strength of the Ca^{2+} stimulus argues against a shift in the Ca^{2+} sensitivity of exocytosis. Third, the unaltered kinetic properties of the remaining secretion and the normal rise times and half-widths of single amperometric spikes in the mutants argue against a significant role in the final stage of the fusion process, in contrast to a recent report (Fisher et al., 2001). Fourth, the unaltered charge of single amperometric spikes and the unaltered total number of LDCVs argue against a role in vesicle biogenesis or loading with catecholamine.

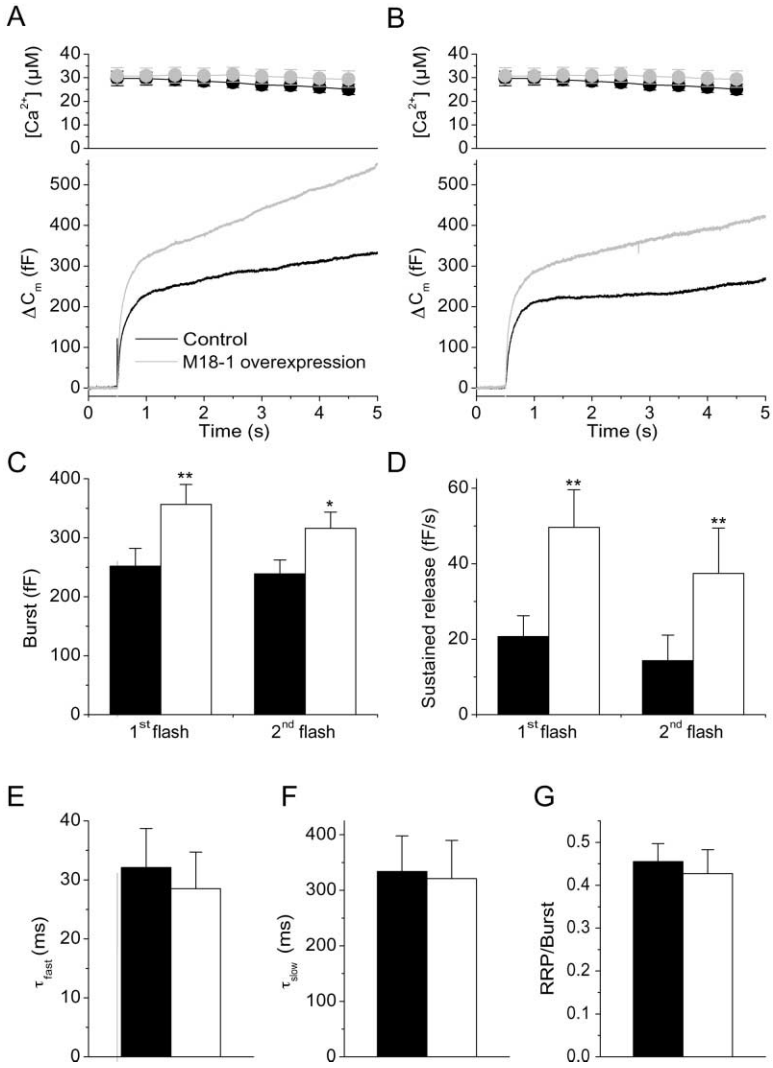

Figure 6. Increased Exocytosis in Bovine Chromaffin Cells Overexpressing Munc18-1

(A) Average intracellular Ca^{2+} concentration (top) and ΔC_m in response to the first flash in control (n = 19; black line and symbols) and Munc18-1-overexpressing (n = 18; gray line and symbols) cells. The first flash was delivered 120–180 s after establishment of the whole-cell configuration.

(B) Average intracellular Ca^{2+} concentration and ΔC_m in response to the second flash for the same cells as in (A). The second flash was applied 120 s after the first flash.

(C) Comparison of the exocytic burst in control and Munc18-1-overexpressing cells.

(D) Comparison of the rate of sustained release in control and Munc18-1-overexpressing cells.

(E and F) Comparison of the time constants of the fast (E) and slow (F) kinetic component of the burst.

(G) Average contribution of the fast component (RRP) to the exocytic burst in control and Munc18-1-overexpressing cells.

(C–G) Solid bars represent controls, and open bars represent Munc18-1-overexpressing cells. Error bars indicate the SEM. Significant differences (Student's t test) are indicated (*$p < 0.05$; **$p < 0.01$).

The normal abundance of vesicles in the mutants and their scattered distribution throughout the cell suggests that export from the Golgi is not impaired and that vesicles can be transported from their site of synthesis. In the absence of Munc18-1 and stable docking, vesicles probably diffuse randomly through the cytoplasm, although we cannot exclude that vesicle transport is also affected in the mutants. Taken together, these results indicate that the Munc18-1 null mutation leads to a selective defect in the docking of LDCVs at the target membrane.

As a complementary approach to the Munc18-1-deficient chromaffin cells, we overexpressed the protein in isolated bovine chromaffin cells, using the Semliki Forest Virus expression system (Ashery et al., 1999). The observed effect of Munc18-1 overexpression was reminiscent of the effect of overexpression of Munc13-1 (Ashery et al., 2000), since both proteins lead to an increased amount of fusion-competent vesicles without affecting the kinetics of vesicle fusion. However, Munc13-1 overexpression leads to a 3-fold increase in the exocytic response to the first flash and a strongly suppressed response to a second flash (Ashery et al., 2000). In contrast, Munc18-1 overexpression causes a relatively mild increase in the response to the first flash (~140% of control), but this increase persists during the second and even later flashes. These findings can be explained assuming that Munc18-1 acts upstream of Munc13-1, the former as a regulator of LDCV docking and the latter as priming factor promoting the transition of LDCVs from a docked but fusion-incompetent state to fusion competence. Indeed, if priming is stimulated, an unusually large fraction of the total pool of docked LDCVs will fuse in response to the first flash. Thereafter, the pool of docked vesicles is severely depleted, and, because docking is relatively slow, the response to the second flash will be suppressed (Ashery et al., 2000). If, in contrast, the docking reaction is stimulated, the larger pool of docked LDCVs indirectly results in more fusion-competent vesicles and thus a larger first flash response. However, after the first flash, a sufficient number of docked vesicles will remain to supply the releasable pools, giving rise to robust responses to subsequent flashes.

Although our present findings are strongly indicative of a critical role for Munc18-1 in LDCV docking, alternative explanations need to be considered. A first alterna-

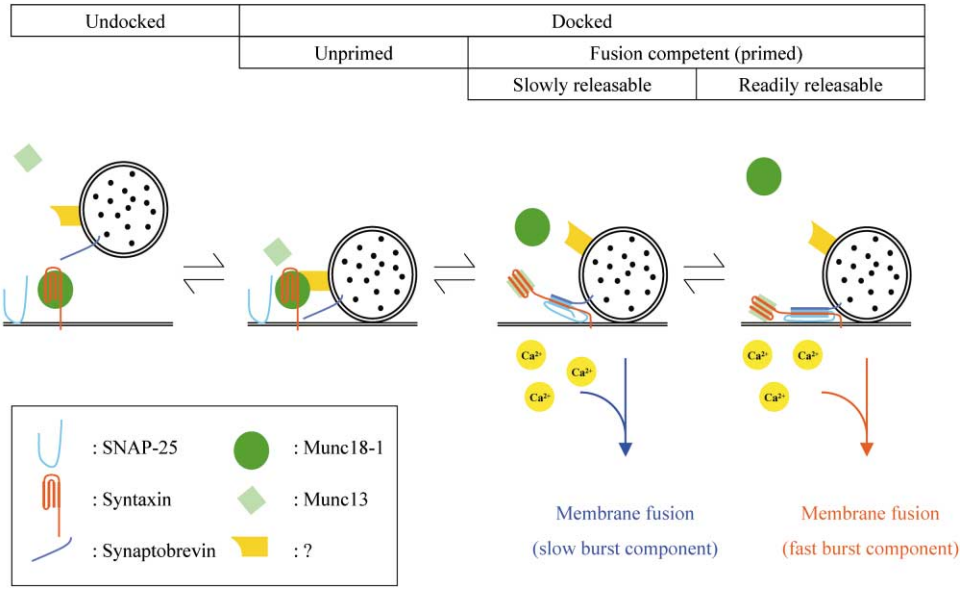

Figure 7. Model for the Role of Munc18-1 in LDCV Secretion

The Munc18-1-Syntaxin-1 complex on the plasma membrane enables the docking of an LDCV at the plasma membrane. Docking involves an unidentified vesicular recognition factor (in yellow). After docking, Munc18-1 detaches from Syntaxin-1. Syntaxin-1 can then assume an open configuration, which allows the interaction with Synaptobrevin/VAMP (on the vesicle) and SNAP-25 (at the plasma membrane) leading to *trans*-SNARE complex formation. Binding of Munc-13 to the N terminus of Syntaxin-1 stabilizes its open configuration and thereby promotes SNARE complex formation. Once the *trans*-SNARE complex is formed, the vesicle reaches the fusion-competent, primed state. Two fusion-competent states are discriminated, corresponding to the slowly releasable pool (SRP) and the readily releasable pool (RRP), which differ in their Ca^{2+}-dependent fusion kinetics. These two states may arise from the interconversion between loosely and tightly assembled SNARE complexes. See text for more details and references.

tive is that the defective LDCV docking in the mutants is an indirect consequence of a defective innervation of the adrenal. This may be assumed because neurotransmission is abolished in the CNS of these mice (Verhage et al., 2000). However, this explanation is improbable for several reasons. First, functional cholinergic innervation of the adrenal medulla by the splanchnic nerve is absent in newborn rodents and does not fully develop until the first postnatal weeks (Slotkin et al., 1980). Thus, neither null mutant nor control chromaffin cells are innervated at the stage at which all experiments were performed. Second, chromaffin cells are fully capable of releasing catecholamine before they get innervated, indicating that the fusion machinery for LDCV secretion does not require nerve stimulation to become functional (Rosenthal and Slotkin, 1977). Third, the observed defects in the mutant were specific, i.e., gross morphology of chromaffin cells and many aspects of their physiology were normal. Fourth, electron micrographs of LDCV-secreting pituitary somatotrophs revealed a similar phenotype (N. Korteweg, personal communication), indicating that the docking defect is a general and specific consequence of the Munc18-1 deletion in LDCV-secreting cells.

A second alternative is that the effects in the null mutant and overexpressing cells are not directly caused by changes in the expression level of Munc18-1 itself but by concomitant changes in Syntaxin-1 levels. Although we cannot completely rule out that the lower Syntaxin-1 levels partially contribute to the reduced secretion in the Munc18-1-deficient cells, it appears unlikely that a 2-fold reduction in Syntaxin-1 levels would cause a 10-fold reduction in LDCV docking and secretion. Moreover, PC12 cells in which Syntaxin-1 levels were reduced displayed an increase in LDCV release (Watanabe et al., 1999). Likewise, the enhanced secretion in Munc18-1-overexpressing cells is not likely to be a consequence of increased Syntaxin-1 levels. First, there were no detectable changes in Syntaxin-1 levels in the Munc18-1-overexpressing chromaffin cells. Second, overexpression of Syntaxin-1 has by itself an inhibitory rather than a stimulatory effect on LDCV secretion (Fujita et al., 1998).

What then is the mechanism whereby Munc18-1 regulates the docking of LDCVs at the plasma membrane? In the absence of Munc18-1, almost no LDCVs were found within 25 nm from the plasma membrane. Since the distance between vesicle and plasma membrane most likely needs to be less than 25 nm (i.e., twice the length of the four-helix bundle of the SNARE complex [Sutton et al., 1998]) to allow vesicle and target membrane SNARE proteins to interact, this strongly indicates that the defect in the null mutants is upstream of SNARE complex assembly. Based on our present findings and on results from earlier studies on the function of SNARE proteins and their interacting molecules, we propose the following model (Figure 7). Munc18-1 and Syntaxin-1 in its closed configuration form a complex on the plasma membrane that is mutually exclusive of the SNARE complex (Pevsner et al., 1994a; Dulubova et al., 1999; Yang et al., 2000; Misura et al., 2000). We suggest that this complex functions as a recognition platform that facili-

tates docking of LDCVs at the plasma membrane. The vesicular factor that recognizes the Munc18-1-Syntaxin-1 complex could be a Rab-Rab effector complex (Dascher et al., 1991) or one of the proteins known to interact with Munc18-1, such as Mint (Okamoto and Sudhof, 1997), Doc2 (Verhage et al., 1997), or Munc13 (Sassa et al., 1999). After docking, Munc18-1 is released from Syntaxin-1, which allows the latter protein to assume an open configuration (Dulubova et al., 1999). In this open form, Syntaxin-1 can interact with SNAP-25 and Synaptobrevin to form a *trans*-SNARE complex. SNARE complex formation is enhanced by Munc13-1, which binds to the N-terminal end of Syntaxin-1 and thereby stabilizes its open configuration (Brose et al., 2000). Vesicles linked to the plasma membrane by *trans*-SNARE complexes are referred to as primed and only require an increase in $[Ca^{2+}]_i$ to undergo fusion. Two distinct pools of fusion-competent vesicles can be distinguished based on differences in Ca^{2+}-dependent fusion kinetics (Voets et al., 1999; Voets, 2000) and may correspond to vesicles with either loose or tight *trans*-SNARE complexes (Xu et al., 1999).

We found that overexpression of Munc18-1 stimulates LDCV secretion, which contrasts with previous studies showing that introducing additional SM protein had either no effect (Graham et al., 1997) or even an inhibitory effect (Schulze et al., 1994; Dresbach et al., 1998) on regulated exocytosis. These apparently conflicting data could be indicative of important differences in the molecular regulation of secretion between different neurosecretory preparations. Alternatively, the release of SM protein from Syntaxin-1, which is required for the initialization of SNARE complex formation (Dulubova et al., 1999), may be rate limiting in certain cell types. Introducing additional SM protein in these cells might hold most Syntaxin-1 molecules complexed in the closed configuration (Figure 7), thereby hindering SNARE complex formation and vesicle fusion.

Our results demonstrate that chromaffin cells lacking Munc18-1 are still capable of mediating LDCV docking and fusion, albeit at strongly reduced rates. In contrast, no residual secretory activity could be detected in *S. cerevisiae* Sec1p mutants (Novick et al., 1980), and synaptic transmission was completely inhibited in mouse Munc18-1 null mutants (Verhage et al., 2000). Interestingly, the electrophysiological data suggest that the phenotype of Munc18-1 null mutants in chromaffin cells is less severe than in the CNS, whereas the morphological data suggest the opposite. Indeed, Munc18-1-deficient synapses, although incapable of releasing neurotransmitter, contained normal amounts of morphologically docked synaptic vesicles (Verhage et al., 2000). This may indicate that Munc18-1-deficient CNS synapses possess additional mechanisms to secure targeting of synaptic vesicles to the active zone. However, the absence of synaptic transmission in these synapses implies that such Munc18-1-independent docking is nonfunctional.

In conclusion, our data demonstrate that Munc18-1 is an important, positive regulator of LDCV secretion and indicate that it plays a crucial role at the docking step, before *trans*-SNARE complexes have assembled. These findings imply that Munc18-1 functions upstream of Munc13, which is involved in the priming of already docked vesicles (Ashery et al., 2000; Brose et al., 2000), and of ComplexinI/II and Synaptotagmin I, which are thought to play a role after vesicle priming in the Ca^{2+}-dependent fusion reaction (Reim et al., 2001; Tokumaru et al., 2001; Geppert et al., 1994). Given their widespread expression in all eukaryotic cell types, we speculate that other SM proteins perform a similar role in a variety of intracellular vesicle trafficking systems.

Experimental Procedures

Chromaffin Cell Preparation

Mouse embryos at embryonic day 18 (E18) were obtained by caesarean section of pregnant females from timed heterozygous matings (Verhage et al., 2000). Adrenal glands were removed, and slices of 80–100 μm thickness were prepared as previously described (Moser and Neher, 1997). Since no obvious differences in LDCV secretion were observed between wild-type (+/+) and heterozygous (+/−) embryos, data from these animals were pooled and classified as control. Slices were used starting shortly after cutting for 4–6 hr.

Isolated bovine adrenal chromaffin cells were prepared and transfected as described previously (Ashery et al., 1999).

Whole-Cell Capacitance Measurements

Conventional whole-cell recordings were performed with 3–4 MΩ pipettes, and an EPC-9 patch-clamp amplifier together with Pulse software (HEKA, Lambrecht, Germany) was used. The pipette solution contained (in mM) Cs-glutamate, 110; NaCl, 8; Mg-ATP, 2; Na_2-GTP, 0.3; Cs-HEPES, 20; nitrophenyl-EGTA (NP-EGTA), 5; $CaCl_2$, 3.5; Furaptra, 0.3; and Fura-2, 0.2 (pH 7.2). Adrenal slices were bathed in a solution containing NaCl, 125; $NaHCO_3$, 26; KCl, 2.5; NaH_2PO_4, 1.25; $CaCl_2$, 2; $MgCl_2$, 1; glucose, 10; and d-tubocurarine, 0.2; bubbled to pH 7.4 with 95% O_2 and 5% CO_2. Isolated chromaffin cells were bathed in a solution containing NaCl, 140; KCl, 2.8; $CaCl_2$, 2; $MgCl_2$, 1; Na-HEPES, 10; and glucose, 10 (pH 7.4).

Capacitance measurements were performed using the Lindau-Neher technique implemented as the "sine + dc" mode of the "software lock-in" extension of PULSE software. A 1 kHz, 70mV peak-to-peak sinusoid stimulus was applied about a DC holding potential of −80mV. All experiments were performed at room temperature.

Amperometry

Carbon fiber electrodes were prepared from 10 μM diameter fibers (Amoco Performance Products, Greenville, SC) as described (Schulte and Chow, 1996). A constant voltage of 780mV versus Ag/AgCl reference was applied to the electrode, whose tip was gently pressed against the cell surface. The amperometric current was sampled at 10 kHz and digitally filtered at 500 Hz.

Measurements of $[Ca^{2+}]_i$ and Photolysis of Caged Ca^{2+}

$[Ca^{2+}]_i$ was measured using a mixture of two indicator dyes, Fura-2 and Furaptra. The dyes were excited with light alternated between 350 and 380 nm using a monochromator-based system (TILL Photonics, Planegg, Germany), and the fluorescent signal was measured using a photomultiplier. To convert the ratio R of the fluorescent signals at both wavelengths into $[Ca^{2+}]_i$, an in vivo calibration curve was used, as previously described (Voets, 2000).

To obtain step-wise increases in $[Ca^{2+}]_i$, short flashes of ultraviolet light from a xenon arc flash lamp (Rapp OptoElectronics, Hamburg, Germany) were applied to the whole cell. The monochromator light was not only used to measure $[Ca^{2+}]_i$ but also allowed to adjust $[Ca^{2+}]_i$ before and after a flash by photolysing smaller amounts of NP-EGTA.

Electron Microscopy

Adrenal glands were removed from control and Munc18-1 null mutant littermates at embryonic day 18 and fixed for 2.5 hr at room temperature with 2% paraformaldehyde, 3% glutaraldehyde, and 1% acrolein in 0.1 M cacodylate buffer (pH 7.2) containing 2.5% DMSO. Adrenals were then washed two times for 15 min with 0.1 M cacodylate buffer (pH 7.2), postfixed for 2 hr at room temperature with 1% OsO_4 in 0.1 M cacodylate buffer (pH 7.2), dehydrated

through a series of increasing ethanol concentrations, and embedded in Epon. Ultrathin sections were collected on formvar-coated copper grids and stained with lead citrate and uranyl acetate.

For each genotype, the distribution of LDCVs was analyzed in sections of 60 randomly selected chromaffin cells from three different animals (and three different grids per animal) at low magnification in the JEOL 1010 electron microscope and subsequently examined at 20,000× magnification. LDCVs were recognized by their round, dense core and had a diameter of approximately 90 nm.

Electrophoresis and Immunoblotting

Adrenal glands were collected at E18 and homogenized in SDS-PAGE loading buffer (66mM Tris/HCl [pH 6.8], 3% [w/v] SDS, 5% [v/v] glycerol, 2% [v/v] β-mercaptoethanol, and 0.001% [w/v] bromophenol blue). SDS-PAGE was performed with two adrenals per lane using 11% gels in Tris-glycine electrophoresis buffer. For Munc18-1 and Munc18c detection, four adrenals per lane were loaded on a 9% gel. Proteins were transferred to PVDF membranes at 100V for 1 hr and detected with either secondary antibodies coupled to horseradish peroxidase and enhanced chemiluminescence or alkaline phosphatase-conjugated secondary antibodies and enhanced chemifluorescence. Quantification was performed on a Fluor S Multilmager (BIO-RAD, Tokyo, Japan).

Antibodies

Monoclonal antibodies against CaM Kinase II and Munc18-1 were purchased from Transduction Laboratories (Lexington, KY). The monoclonal anti-Syntaxin-1A/B (HPC-1) was purchased from Sigma (St. Louis, MO) and the monoclonal anti-SNAP-25 (SMI81) from Sternberger Monoclonals Inc. (Lutherville, MD). The monoclonal antibody against Synaptobrevin/VAMP (Cl69.1; Edelmann et al., 1995), the polyclonal anti-VCP (K331; Sugita and Sudhof, 2000), and the polyclonal anti-Munc18c (Tellam et al., 1995) were as described previously. The horseradish peroxidase-conjugated secondary antibody against mouse IgG was purchased from Jackson Immuno Research Laboratories, Inc. (West Grove, PA), and the peroxidase-conjugated secondary anti-rabbit IgG was from Sigma. The ECL-substrate (Super Signal West Dura Extended) was purchased from Pierce (Rockford, IL). The alkaline phosphatase-conjugated secondary mouse and rabbit IgG and IgM and ECF-substrate were purchased from Amersham (Buckinghamshire, UK).

Acknowledgments

We thank Anke Bührmann, Michael Pilot, Robbert Zalm, and Danielle Dam for excellent technical assistance; and Dr. Uri Ashery for discussion and assistance with the virus transfection. This work was supported by grants from the Deutsche Forschungsgemeinschaft (SFB 523) and the Netherlands Organization for Scientific Research (NWO). T.V. is a postdoctoral Fellow of the Fund for Scientific Research—Flanders (Belgium) (F.W.O.-Vlaanderen). R.F.T. was supported by the NWO-GBMW 903-42-023, E.C.B. by NWO-GBMW 903-42-095, and H.D.W. by NWO-GpD 970-10-036.

Received June 8, 2001; revised June 15, 2001.

References

Ashery, U., Betz, A., Xu, T., Brose, N., and Rettig, J. (1999). An efficient method for infection of adrenal chromaffin cells using the Semliki Forest virus gene expression system. Eur. J. Cell Biol. *78*, 525–532.

Ashery, U., Varoqueaux, F., Voets, T., Betz, A., Thakur, P., Koch, H., Neher, E., Brose, N., and Rettig, J. (2000). Munc13-1 acts as a priming factor for large dense-core vesicles in bovine chromaffin cells. EMBO J. *19*, 3586–3596.

Augustine, G.J., Burns, M.E., DeBello, W.M., Hilfiker, S., Morgan, J.R., Schweizer, F.E., Tokumaru, H., and Umayahara, K. (1999). Proteins involved in synaptic vesicle trafficking. J. Physiol. *520*, 33–41.

Bennett, M.K., and Scheller, R.H. (1993). The molecular machinery for secretion is conserved from yeast to neurons. Proc. Natl. Acad. Sci. USA *90*, 2559–2563.

Brose, N., Rosenmund, C., and Rettig, J. (2000). Regulation of transmitter release by Unc-13 and its homologues. Curr. Opin. Neurobiol. *10*, 303–311.

Brunger, A.T. (2000). Structural insights into the molecular mechanism of Ca^{2+}-dependent exocytosis. Curr. Opin. Neurobiol. *10*, 293–302.

Carr, C.M., Grote, E., Munson, M., Hughson, F.M., and Novick, P.J. (1999). Sec1p binds to SNARE complexes and concentrates at sites of secretion. J. Cell Biol. *146*, 333–344.

Chen, Y.A., and Scheller, R.H. (2001). SNARE-mediated membrane fusion. Nat. Rev. Mol. Cell Biol. *2*, 1–9.

Chen, Y.A., Scales, S.J., Patel, S.M., Doung, Y.C., and Scheller, R.H. (1999). SNARE complex formation is triggered by Ca^{2+} and drives membrane fusion. Cell *97*, 165–174.

Chow, R.H., von Ruden, L., and Neher, E. (1992). Delay in vesicle fusion revealed by electrochemical monitoring of single secretory events in adrenal chromaffin cells. Nature *356*, 60–63.

Dascher, C., Ossig, R., Gallwitz, D., and Schmitt, H.D. (1991). Identification and structure of four yeast genes (SLY) that are able to suppress the functional loss of YPT1, a member of the RAS superfamily. Mol. Cell. Biol. *11*, 872–885.

Dresbach, T., Burns, M.E., O'Connor, V., DeBello, W.M., Betz, H., and Augustine, G.J. (1998). A neuronal Sec1 homolog regulates neurotransmitter release at the squid giant synapse. J. Neurosci. *18*, 2923–2932.

Dulubova, I., Sugita, S., Hill, S., Hosaka, M., Fernandez, I., Sudhof, T.C., and Rizo, J. (1999). A conformational switch in syntaxin during exocytosis: role of munc18. EMBO J. *18*, 4372–4382.

Edelmann, L., Hanson, P.I., Chapman, E.R., and Jahn, R. (1995). Synaptobrevin binding to synaptophysin: a potential mechanism for controlling the exocytotic fusion machine. EMBO J. *14*, 224–231.

Fernandez-Chacon, R., and Südhof, T.C. (1999). Genetics of synaptic vesicle function: toward the complete functional anatomy of an organelle. Annu. Rev. Physiol. *61*, 753–776.

Fisher, R.J., Pevsner, J., and Burgoyne, R.D. (2001). Control of fusion pore dynamics during exocytosis by Munc18. Science *291*, 875–878.

Fujita, Y., Shirataki, H., Sakisaka, T., Asakura, T., Ohya, T., Kotani, H., Yokoyama, S., Nishioka, H., Matsuura, Y., Mizoguchi, A., et al. (1998). Tomosyn: a syntaxin-1-binding protein that forms a novel complex in the neurotransmitter release process. Neuron *20*, 905–915.

Geppert, M., Goda, Y., Hammer, R.E., Li, C., Rosahl, T.W., Stevens, C.F., and Südhof, T.C. (1994). Synaptotagmin I: a major Ca^{2+} sensor for transmitter release at a central synapse. Cell *79*, 717–727.

Gorgas, K., and Böck, P. (1976). Morphology and histochemistry of the adrenal medulla. Histochemistry *50*, 17–31.

Grabowski, R., and Gallwitz, D. (1997). High-affinity binding of the yeast cis-Golgi t-SNARE, Sed5p, to wild-type and mutant Sly1p, a modulator of transport vesicle docking. FEBS Lett. *411*, 169–172.

Graham, M.E., Sudlow, A.W., and Burgoyne, R.D. (1997). Evidence against an acute inhibitory role of nSec-1 (munc-18) in late steps of regulated exocytosis in chromaffin and PC12 cells. J. Neurochem. *69*, 2369–2377.

Harrison, S.D., Broadie, K., van de Goor, J., and Rubin, G.M. (1994). Mutations in the *Drosophila Rop* gene suggest a function in general secretion and synaptic transmission. Neuron *13*, 555–566.

Hata, Y., Slaughter, C.A., and Sudhof, T.C. (1993). Synaptic vesicle fusion complex contains unc-18 homologue bound to syntaxin. Nature *366*, 347–351.

Hay, J.C., and Scheller, R.H. (1997). SNAREs and NSF in targeted membrane fusion. Curr. Opin. Cell Biol. *9*, 505–512.

Jahn, R. (2000). Sec1/Munc18 proteins: mediators of membrane fusion moving to center stage. Neuron *27*, 201–204.

Lin, R.C., and Scheller, R.H. (2000). Mechanisms of synaptic vesicle exocytosis. Annu. Rev. Cell Dev. Biol. *16*, 19–49.

Misura, K.M., Scheller, R.H., and Weis, W.I. (2000). Three-dimensional structure of the neuronal-Sec1-syntaxin 1a complex. Nature *404*, 355–362.

Morgan, A., and Burgoyne, R.D. (1997). Common mechanisms for regulated exocytosis in the chromaffin cell and the synapse. Seminars Cell Dev. Biol. *8*, 141–149.

Moser, T., and Neher, E. (1997). Rapid exocytosis in single chromaffin cells recorded from mouse adrenal slices. J. Neurosci. *17*, 2314–2323.

Neher, E. (1998). Vesicle pools and Ca^{2+} microdomains: new tools for understanding their roles in neurotransmitter release. Neuron *20*, 389–399.

Nichols, B.J., Holthuis, J.C., and Pelham, H.R. (1998). The Sec1p homologue Vps45p binds to the syntaxin Tlg2p. Eur. J. Cell Biol. *77*, 263–268.

Niemann, H., Blasi, J., and Jahn, R. (1994). Clostridial neurotoxins: new tools for dissecting exocytosis. Trends Cell Biol. *4*, 179–185.

Novick, P., Field, C., and Schekman, R. (1980). Identification of 23 complementation groups required for post-translational events in the yeast secretory pathway. Cell 21, 205–215.

Okamoto, M., and Sudhof, T.C. (1997). Mints, Munc18-interacting proteins in synaptic vesicle exocytosis. J. Biol. Chem. *272*, 31459–31464.

Pevsner, J., Hsu, S.C., Braun, J.E., Calakos, N., Ting, A.E., Bennett, M.K., and Scheller, R.H. (1994a). Specificity and regulation of a synaptic vesicle docking complex. Neuron *13*, 353–361.

Pevsner, J., Hsu, S.C., and Scheller, R.H. (1994b). n-Sec1: a neural-specific syntaxin-binding protein. Proc. Natl. Acad. Sci. USA *91*, 1445–1449.

Reim, K., Mansour, M., Varoqueaux, F., McMahon, H.T., Sudhof, T.C., Brose, N., and Rosenmund, C. (2001). Complexins regulate a late step in Ca2+-dependent neurotransmitter release. Cell *104*, 71–81.

Robinson, L.J., and Martin, T.F. (1998). Docking and fusion in neurosecretion. Curr. Opin. Cell Biol. *10*, 483–492.

Rosenthal, R.N., and Slotkin, T.A. (1977). Development of nicotinic responses in the rat adrenal medulla and long-term effects of neonatal nicotine administration. Br. J. Pharmacol. *60*, 59–64.

Sassa, T., Harada, S., Ogawa, H., Rand, J.B., Maruyama, I.N., and Hosono, R. (1999). Regulation of the UNC-18-Caenorhabditis elegans syntaxin complex by UNC-13. J. Neurosci. *19*, 4772–4777.

Schulte, A., and Chow, R.H. (1996). A simple method for insulating carbon-fiber microelectrodes using anodic electrophoretic deposition of paint. Anal. Chem. *68*, 3054–3058.

Schulze, K.L., Littleton, J.T., Salzberg, A., Halachmi, N., Stern, M., Lev, Z., and Bellen, H.J. (1994). rop, a *Drosophila* homolog of yeast Sec1 and vertebrate n-Sec1/Munc-18 proteins, is a negative regulator of neurotransmitter release in vivo. Neuron *13*, 1099–1108.

Slotkin, T.A., Smith, P.G., Lau, C., and Bareis, D.L. (1980). Functional aspects of development of catecholamine biosynthesis and release in the sympathetic nervous system. In Biogenic Amines in Development, H. Parvez and S. Parvez, eds. (Amsterdam: Elsevier), pp. 29–48.

Sollner, T., Bennett, M.K., Whiteheart, S.W., Scheller, R.H., and Rothman, J.E. (1993). A protein assembly-disassembly pathway in vitro that may correspond to sequential steps of synaptic vesicle docking, activation, and fusion. Cell *75*, 409–418.

Steyer, J.A., Horstmann, H., and Almers, W. (1997). Transport, docking and exocytosis of single secretory granules in live chromaffin cells. Nature *388*, 474–478.

Sugita, S., and Sudhof, T.C. (2000). Specificity of Ca2+-dependent protein interactions mediated by the C2A domains of synaptotagmins. Biochemistry *39*, 2940–2949.

Sutton, R.B., Fasshauer, D., Jahn, R., and Brunger, A.T. (1998). Crystal structure of a SNARE complex involved in synaptic exocytosis at 2.4 Å resolution. Nature *395*, 347–353.

Tellam, J.T., McIntosh, S., and James, D.E. (1995). Molecular identification of two novel Munc-18 isoforms expressed in non-neuronal tissues. J. Biol. Chem. *270*, 5857–5863.

Tokumaru, H., Umayahara, K., Pellegrini, L.L., Ishizuka, T., Saisu, H., Betz, H., Augustine, G.J., and Abe, T. (2001). SNARE complex oligomerization by synaphin/complexin is essential for synaptic vesicle exocytosis. Cell *104*, 421–432.

Verhage, M., de Vries, K.J., Roshol, H., Burbach, J.P., Gispen, W.H., and Sudhof, T.C. (1997). DOC2 proteins in rat brain: complementary distribution and proposed function as vesicular adapter proteins in early stages of secretion. Neuron *18*, 453–461.

Verhage, M., Maia, A.S., Plomp, J.J., Brussaard, A.B., Heeroma, J.H., Vermeer, H., Toonen, R.F., Hammer, R.E., van den Berg, T.K., Missler, M., et al. (2000). Synaptic assembly of the brain in the absence of neurotransmitter secretion. Science *287*, 864–869.

Voets, T. (2000). Dissection of three Ca^{2+}-dependent steps leading to secretion in chromaffin cells from mouse adrenal slices. Neuron *28*, 537–545.

Voets, T., Neher, E., and Moser, T. (1999). Mechanisms underlying phasic and sustained secretion in chromaffin cells from mouse adrenal slices. Neuron *23*, 607–615.

Watanabe, T., Fujiwara, T., Komazaki, S., Yamaguchi, K., Tajima, O., and Akagawa, K. (1999). HPC-1/syntaxin 1A suppresses exocytosis of PC12 cells. J. Biochem. *125*, 685–689.

Weber, T., Zemelman, B.V., McNew, J.A., Westermann, B., Gmachl, M., Parlati, F., Sollner, T.H., and Rothman, J.E. (1998). SNAREpins: minimal machinery for membrane fusion. Cell *92*, 759–772.

Xu, T., Rammner, B., Margittai, M., Artalejo, A.R., Neher, E., and Jahn, R. (1999). Inhibition of SNARE complex assembly differentially affects kinetic components of exocytosis. Cell *99*, 713–722.

Yang, B., Steegmaier, M., Gonzalez, L.C., Jr., and Scheller, R.H. (2000). nSec1 binds a closed conformation of syntaxin1A. J. Cell Biol. *148*, 247–252.

Zucker, R.S. (1996). Exocytosis: a molecular and physiological perspective. Neuron *17*, 1049–1055.